

# Towards Autonomous Crop-Agnostic Visual Navigation in Arable Fields

Alireza Ahmadi, Michael Halstead, and Chris McCool

**Abstract**—Autonomous navigation of a robot in agricultural fields is essential for every task from crop monitoring through to weed management and fertilizer application. Many current approaches rely on accurate GPS, however, such technology is expensive and also prone to failure (e.g. through lack of coverage). As such, navigation through sensors that can interpret their environment (such as cameras) is important to achieve the goal of autonomy in agriculture.

In this paper we introduce a purely vision based navigation scheme which is able to reliably guide the robot through row-crop fields. Independent of any global localization or mapping, this approach is able to accurately follow the crop-rows and switch between the rows, only using on-board cameras. With the help of a novel crop-row detection and a novel crop-row switching technique, our navigation scheme can be deployed in a wide range of fields with different canopy types in various growth stages. We have extensively tested our approach in five different fields under various illumination conditions using our agricultural robotic platform (BonnBot-I). And our evaluations show that we have achieved a navigation accuracy of 3.82cm over five different crop fields.

**Keywords** — Robotics and Automation in Agriculture and Forestry; Agricultural Automation; Vision-Based Navigation.

## I. INTRODUCTION

Novel agricultural robotic technologies need to ensure they meet the needs of the key stakeholder, farmers. Usually, this means being cost effective both as a platform and as a labor (or mechanical) replacement technology. However, another critical element is that the technology can be deployed to a variety of fields and environmental conditions with minimal intervention (supervision) from the farmer. In particular, navigating through the field is central to the real-world deployment of agricultural robotics.

Hence, automated field navigation for a robot is essential for every task. For autonomous navigation it is common for platforms to use precise real-time kinematic (RTK) GNSS as it is being used in fully controlled and engineered agricultural sites where they heavily rely on structural information [1], [2]. But, robotic technologies will never be guaranteed accurate GPS in every field, first due to its expense and second because of the coverage. Since, currently most of fields seeding is completed using traditional approaches without the use of auto-seeding geo-referenced systems, creating a gap between GPS capabilities and farming requirements [1]. As such, utilizing GPS technology in unregistered fields increases the risk of damaging crops [3]. Therefore, generally applicable methods to navigate the field, such as local crop-row following, are required.

All authors are with the University of Bonn, Bonn 53115 Germany. {alireza.ahmadi, michael.halstead, cmccool}@uni-bonn.de

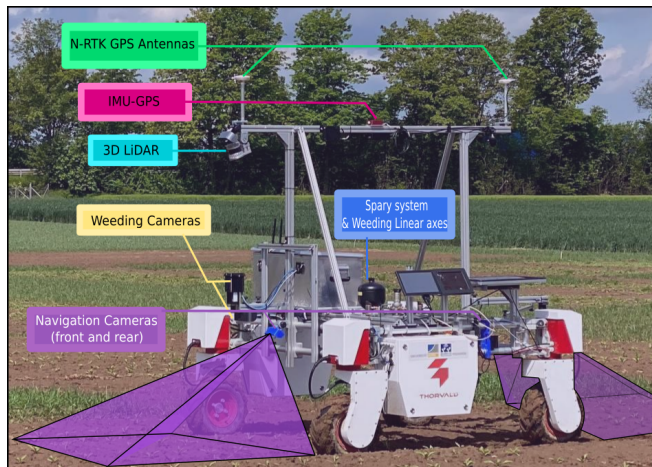


Fig. 1: An overview of BonnBot-I autonomously following lanes of crops using two symmetrically mounted monocular camera in front and back.

In our prior work [4] we introduced a GPS independent technique that was able to traverse a single crop-row and switch between adjacent rows. However, the prior work was only applicable to a single crop-row system which is inefficient and does not take advantage of the overall planting structure in the field. For instance, normally multiple crop-rows are planted in a lane for the platform (robot or tractor) to traverse; a lane consists of multiple crop-rows.

In this paper we introduce a novel crop-agnostic vision based navigation scheme as illustrated in Fig. 1. Our method is capable of extracting repetitive patterns in row-crop fields and navigates along multiple crop-rows. It utilizes a novel feature based crop-row switching mechanism that enables the robot to autonomously and reliably change between the lanes. The system presented in this paper is deployed on BonnBot-I for a variety of row-crops and provides the following contributions:

- a robust multi-crop-row detection strategy, capable of dealing with cluttered and weedy scenes for a variety of crop types;
- a crop-agnostic crop-row following approach which enables autonomous guidance evaluated on a robot (BonnBot-I) in the field; and
- a multi-crop-row lane switching strategy which enables BonnBot-I to switch to a new lane independent of any global positioning system.

These approaches are evaluated in real-world fields and we plan to open-source our implementation for usage by the community.

## II. RELATED WORK

Autonomous agricultural robots could improve productivity [5], enable targeted field interventions [6] and facilitate crop monitoring [7]. For uptake of these platforms they should be deploy-able in a variety of scenarios including different cultivars, crop-row structures, and seeding patterns [8]. A key enabling technology is reliable navigation through the whole field [9], [10].

One potential solution to the navigation problem is to make use of the Global Navigation Satellite System (GNSS). Such an approach has been used for both agricultural machinery [11] and robotic platforms [2]. The downside of this approach is that it relies on an expensive sensor and suffers from limitations such as possible GNSS outages and reliance on geo-referenced auto-seeding. Thus, crop-based navigation techniques leveraging the field structure were investigated for autonomous guidance [12], [4] and in-field interventions [13].

In an attempt to use the structure of a field, Barawid *et al.* [14] investigated 2D LiDAR based navigation systems for orchards and a similar strategy was used in a simulated environment by [15] for traversing row-crop fields. While these approaches enable side-applications such as obstacle avoidance, frame drift in self-similar environments can cause issues [16], including crop damage.

To avoid crop damage through GNSS or LiDAR failures, RGB based navigation approaches directly exploit the available visual information. These techniques can vary significantly in terms of cost, algorithm simplicity, and availability. Classical machine vision approaches detect crop-rows with juvenile crops [13] or detect crop-rows under challenging illumination conditions [17]. Other classical approaches include crop stem locations from Multi-spectral images [18], and Plant Stem Emerging Point (PSEP) using hand-crafted features [19]. While these approaches are generally real-time and can, to varying degrees, navigate a lane they do require hand selected features which reduces the learning abilities of the techniques. In recent research deep learning approaches have superseded their traditional counterparts as shown by [20].

Kraemer *et al.* [20] used a deep learning approach to reconcile the PSEP features by exploiting the likelihood maps of a deep neural networks (DNN). Also utilising DNNs, [21] proposed a convolutional neural network (CNN) for strawberry crop-row detection with accurate navigation. Lin *et al.* [22] also showcase the potential of CNNs to reliably navigate a tea field by classifying tea rows. These approaches are often more accurate than their traditional counterparts for detecting or segmenting specific plants. However, in contrast to traditional approaches, CNNs require a significant amount of labelled data and more computational resources both for training and inference, while being less dynamic in nature.

To perform vision based navigation two common approaches exist: proportional-integral-derivative (PID) or visual servoing. Billingsley *et al.* [12] extracted the row of

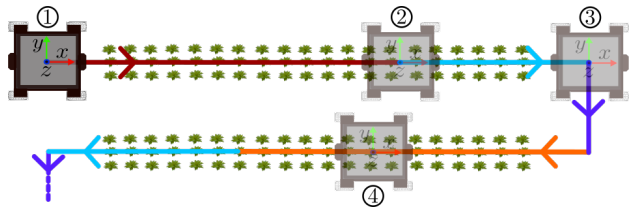


Fig. 2: In-field navigation strategy, (1) following crop rows with front camera, (2) exiting crop rows using back camera, (3) switching to the next crop rows, and (4) following new crop rows with back camera.

plants using a Hough transform, this information was then fed to a PID controller for navigation through a sugar-beet field. The visual-servoing [23] technique was also exploited for autonomous car guidance in urban areas [24] by road lane following with obstacle avoidance using monocular camera. These methods regularize the controlled agents motion within a loop directly based on the current visual features.

The technique proposed in this paper draws inspiration from our previous work [4] where we are able to both navigate a single crop-row and switch lanes at the end. We extend on this work to including being crop agnostic and able to follow multiple crop-rows in a single lane. Also, as real-time performance is important, we rely on traditional machine vision techniques.

## III. AUTONOMOUS NAVIGATION IN ROW-CROP FIELDS

Our navigation strategy is influenced by the robot that we use. In this work we use a retrofitted Thorvald platform [25] which we refer to as BonnBot-I. Below we provide, in brief, the specifications of the BonnBot-I platform and then present the high level guidance strategy of our proposed navigation scheme.

### A. BonnBot-I Platform

BonnBot-I is a prototype crop monitoring and weeding platform. The platform is a lightweight Thorvald system which has been adapted for arable farming and phenotyping fields in Europe. For this, the width of the platform was set to 1.4m wheel-centre-to-wheel-centre with a vertical clearance of 0.86m to ensure the platform could operate in the field during the early growth cycle of most plants. The length of the robot was set to 1.4m ensuring there is room for all the weeding tools, and has a maximum speed of 1.5 m/s. BonnBot-I has multiple sensors, of interest for navigation is a GNSS (with an IMU) and two RGB-D cameras which are mounted equally distant from the center of rotation of the robot symmetrically (in front and back) illustrated in Fig. 1.

### B. In Field Guidance Strategy

A benefit of crop-rows is that they are generally planted in consistent long parallel structures. A downside to this parallel structure is that there is no connection between them. Therefore, the platform needs to not only follow the crop-row without damaging the crop but also autonomously switch between them. To achieve multi-crop-row following

we employ a similar algorithm to our previous work in [4] for a single crop-row.

Fig. 2 outlines our multi-crop-row following strategy. Starting in a corner of the field, the platform autonomously follows the current set of crop-rows (a lane) using vision based navigation techniques ① until the front facing camera detects the end of the current lane. The rear camera then guides the robot to the exit point, end of the lane, actively guiding the robot at all times ②. Using the omni-directional capability, the robot then switches to the next set of crop-rows ③ to be traversed. The benefits of the omni-directional platform again prevails here as we can directly navigate to the new lane without turning around ④, this also outlines the benefit of symmetrically mounted sensors at the front and rear. In the next section we describe the vision-based crop-row following and crop row switching algorithms.

#### IV. VISION-BASED GUIDANCE IN FARMING FIELDS

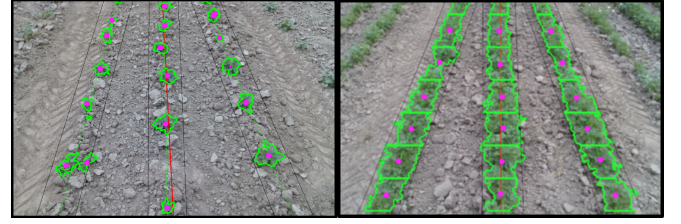
We propose a multi-crop-row following approach that can successfully traverse a row-crop field. Inspired by our prior work on single crop-row following [4], we greatly extend this to achieve multi-crop-row following. In achieving this we have developed a multi-crop-row detection approach described in Sec. IV-A, integrate information from multiple detected crop-rows to perform visual-servoing based crop-row following in Sec. IV-B, and present a multi-crop-row switching approach in Sec. IV-C.

##### A. Multi-Crop-Row Detection

The first step in a successful vision system capable of traversing a field is the assumption that crop-rows are planted in a parallel fashion. To have a completely crop agnostic navigation system the varying distances between the rows for the different crops is an important element. Therefore, it is imperative to have a system that can detect the number of crop rows before instantiating the navigation algorithm.

We perform crop-row detection by employing a sliding window based approach. This extracts the location of the prominent crop-rows while being robust to the appearance of weeds between them. Our detection approach consists of three steps. First, we perform vegetation segmentation followed by connected components operations to find individual regions (plants) and their center points. This allows us to remain agnostic to the crop that has been planted. Second, we automatically detect the number of crop-rows by employing an estimate of the moving-variance which we use to describe the field structure. Finally, we track the detected crop-rows by centering a parallelogram on each row while the robot is traversing the lane. We detail each of these steps below.

1) *Vegetation Mask and Crop Center Extraction:* In the first stage, we summarize a row by the position of the individual plants along it. Each plant is represented by its center point. We obtain this by first computing the vegetation mask of the input RGB image using the Excess Green Index (ExG) [26]. To separate foreground and background pixels in the image based on ExG we employ Otsu's method [27]. Then, each connected component in the vegetation mask is



(a) Lemon-balm

(b) Coriander

Fig. 3: The result of vegetation segmentation (in green) with plant boundaries (in bold green) and the resultant plant centers (magenta dots). In (a) individual plants are easy to see and (b) is a case where crop boundaries have to be estimated.

converted to an object of interest (plant) with the unique center point obtained from the center of mass.

One issue associated with this technique occurs when multiple “plants” are absorbed into a single large region. A single region representing an entire crop-row negatively impacts later stages such as line fitting (described in the next Section). To reconcile this we divide contours into smaller subsections horizontally if they exceed a predefined maximum height, as shown in Fig. 3. Ultimately, this step allows us to cater for a larger variety of canopy types.

2) *Detecting Individual Crop Rows:* Fig. 4 illustrates the crop-row detection algorithm. First, a sliding window  $\Psi$  scans the image from right to left in steps of  $S$ . The size of the sliding window  $w, h$  and the scanning steps  $S$  are set to ensure a large overlap between adjacent steps in the scans. At each step, we compute a line based on crop centers inside the sliding window using least-squares method and find the intersection point  $I_n$  of the line  $L_n$  with the bottom axis of the image. All lines that do not intersect with the bottom of the image are discarded, ensuring that only crop-rows that can impact navigation are included. The estimated intersection  $I_n = [x, y]$  is associated with the angle  $\phi_n$  of corresponding line  $L_n = (I_n, \phi_n)$ .

We use the hypothesized crop lines to represent the local structure of the field and then employ a Moving Variance [28] operator, such that,

$$\sigma^2(\phi_n) = \frac{\sum_{i=n-k/2}^{n+k/2} (\phi_i - \bar{\phi}_n)^2}{k}; \quad \bar{\phi}_n = \frac{\sum_{i=n-k/2}^{n+k/2} \phi_i}{k} \quad (1)$$

where each variance  $\sigma^2(\phi_n)$  is calculated over a sliding window of length  $k$  across neighboring elements of  $\phi_n$ . The moving variance operator yields peaks when there is discord between the local hypothesized crop lines, this occurs between the crop-row lines. Troughs occur when there is consistent agreement regarding the hypothesized crop lines, this occurs in the presence of crop-rows. We refer to this as the field structure signal and is depicted in Fig. 4.

To detect the peaks ( $\blacktriangle$ ) and troughs ( $\nabla$ ) of the field structure signal we use peak prominence with a constant threshold. To detect the troughs, the signal is flipped (via negation) and peak prominence is applied with the same threshold. The detection of troughs is more complex as crop-rows can yield multiple peaks. We resolve this by computing





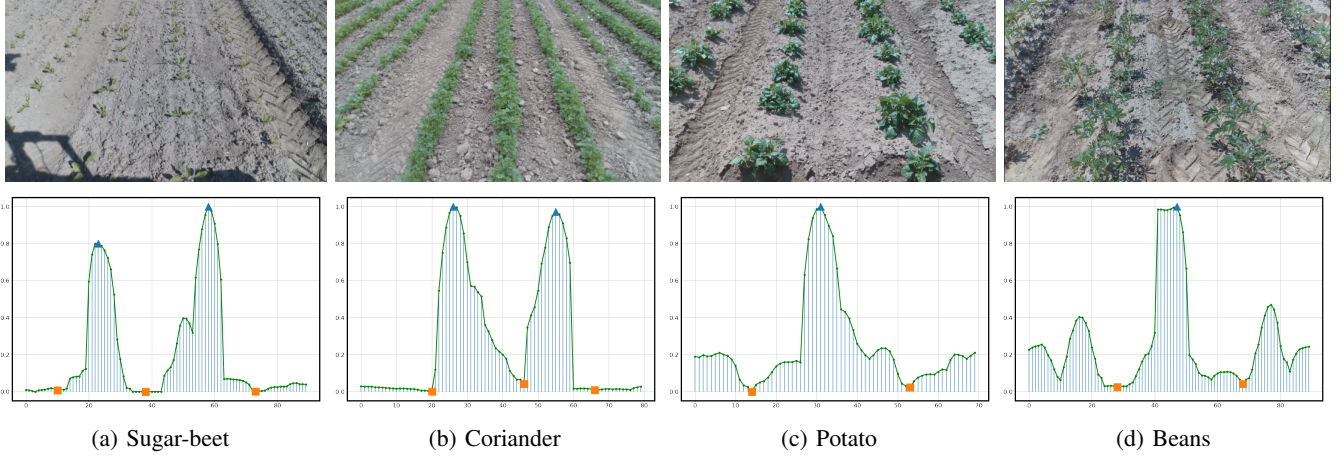


Fig. 6: Illustrations of four crops (top row) with their corresponding field structure signal (bottom row). The detected peaks (blue triangle) and troughs (orange square) obtained via their prominence in the signal are also provided. Denote that, the field structure signal only include the values of lines intersecting with the bottom axes of the image.

matches in  $\Omega$  which are above a threshold  $\lambda$ . This is used to provide a distance measure between the two sets of features:

$$D(\mathcal{G}, \mathcal{G}^*) = \frac{1}{m} \sum_{i=1}^m \Omega_m \quad (2)$$

When  $D(\mathcal{G}, \mathcal{G}^*)$  exceeds a threshold  $\tau_c$  we assume a new crop-row has been found,  $\tau_c$  is a crop type specific constant.

## V. EXPERIMENTAL EVALUATIONS

We performed three experiments to show the capability and robustness of our proposed approaches. First, we evaluate the reliability and consistency of our proposed multi-crop-row detection approach by applying it to different fields with varying numbers of crop-rows (per lane) and canopy shapes. Second, we evaluate the navigation accuracy of the robot along several multi-crop-row paths, relying solely on RGB cameras. Finally, the validity of the lane switching technique is analysed, including the ability to detect and switch between different crops using the same approach.

### A. Experimental Setup

All experiments in this section were completed on BonnBot-I at Campus Klein-Altendorf of University of Bonn. To fast track the field experiments we used a 1:1 scale Gazebo simulation model with a realistic field. From this simulation, along with our previous work in [4] for the camera setup, we were able to derive our algorithmic hyper-parameters. On BonnBot-I, the front and back navigation cameras are fixed at a height of  $1.0\text{ m}$  and tilt angle  $\rho = 65^\circ$ . Both camera resolutions are  $1280 \times 720$  with a capture rate of  $15\text{ fps}$ . For all experiments, the width  $w$  of sliding window  $\Psi$  was kept constant  $w = W/10 = 128$  with a height of  $h = 720$  pixels. This window size and  $S = 100$  ensures  $\approx 92\%$  overlap between consecutive sliding windows. Also, we empirically set  $k = 10$  in Eq. (1) which in simulation provided the best trade-off between sample consistency and neighbourhood relationship. As the primary goal of this platform is to perform weeding we set its velocity to be

a constant  $v_x^* = 0.3\text{ m/s}$ . We use differential velocity control within the crop-rows and omni-directional control for switching between the lanes. Our approach is implemented using Python and PyCuda ensuring real-time operation and runs on a user grade computer (Cincose DS-1202).

### B. Multi-Crop-Row Detection

The first experiment is a qualitative analysis on the ability to detect crop-rows in the field using the technique described in Sec. IV-A. The goal of this technique is to exploit the dominant crop locations and accurately detect the best location for traversing a lane (i.e. keeping the crop-rows under the platform). Due to weeds growing between the crop-rows this can be a challenging proposition in real fields.

Fig. 6 depicts four crop types: sugar-beet, coriander, potato, and beans. Due to space limitations we refrained from adding Lemon-balm results in Fig. 6. The illustrated crops have diverse canopy types (see Fig. 6) and are arranged in two different patterns ( $35\text{ cm}$  or  $55\text{ cm}$  between crop rows) leading to either two or three crop-rows to navigate.

In Fig. 6 it can be seen that the crop-rows of beans were the most difficult to detect. This is due to the presence of weeds in the crop-rows and the height of the crop. While this was a difficult crop to detect our detection technique was still able to exploit the crop information to find the crop-rows, denoted by the orange squares in Fig. 6.

For all crops we were able to consistently detect both the peak (no crop-row) and trough (crop-row) locations regardless of the presence of weeds. This is especially evident in coriander where even with the small distance within the crop-row (between the coriander plants) we are still able to detect the crop-rows. This is an example where dividing single large regions into sub-regions is essential.

Sugar-beet, Fig. 6-a, is another interesting use case. Visually it is considerably more difficult to discern the crop locations, however, this technique was still able to extract the required locations (crop-rows). Overall, this technique for crop-row detection successfully located the required troughs

in order to navigate a lane, providing accurate information required for the other stages of our system.

### C. Navigating Along The Crop-Rows

To analyse the performance of our crop-row navigation technique we require accurate ground truth information. To collect the ground truth information the robot was manually driven down each of the row-crop fields for all crop types and stored for later evaluation. The associated GPS measurements are then used as the “correct” position (accurate to 1cm). Even though manual operation can cause some errors we consider this to be an appropriate ground truth to compare to as the crop-rows are not guaranteed to be planted in a straight line.

We investigate the navigation performance on five crops: sugar-beet, coriander, potato, beans, and lemon-balm. This introduces a range of challenges such as being captured under different weather conditions, different weed density, and varying growth stages. Tab. I outlines the performance on these crops. In general these approaches are consistently able to replicate the ground truth (manual) navigation via our novel crop-row navigation technique.

The sugar-beet navigation was the most complicated crop to follow due to a number of challenging factors. First, the early growth stage, as seen in Fig. 6, made it more complicated to detect the crop lines. Secondly, not all of the sugar-beet had germinated and this led to gaps or “dead space” along the rows.

From a navigational perspective the bean crop had a large standard deviation when considering angular error. The weather conditions played a crucial part in this as heavy winds consistently changed the location of the leaves of the crops. This limitation in the navigation technique leads to large angular variations while traversing the lane.

Overall, the average deviation from the ground truth was 3.82cm or approximately 10% of the crop-row distance. This minor fluctuation is sufficient to ensure safe navigation without damaging crops. Finally, due to this navigational accuracy this technique was consistently able to traverse all the crops in the field and not miss any plant within the rows.

### D. Multi-Crop-Row Switching

The third experiment is designed to show the capability of the multi-crop-row switching method introduced in Sec. IV-C. The differentiation between different crop rows in an outdoor environment is the most crucial step in this process.

TABLE I: Lane following performance of BonnBot-I using proposed method in five different crop rows in Campus Klein-Altendorf of University of Bonn.

Crop	Length	Avg. and std. dev. distance to crop rows	Avg. and std. dev. angular error
<i>Beans</i>	52 m	3.49 $\pm$ 2.89 cm	3.73 $\pm$ 3.21 deg
<i>Potato</i>	37 m	2.18 $\pm$ 3.01 cm	4.91 $\pm$ 1.63 deg
<i>Coriander</i>	54 m	2.91 $\pm$ 2.38 cm	2.57 $\pm$ 1.05 deg
<i>Sugar-beet</i>	69 m	8.41 $\pm$ 3.79 cm	3.25 $\pm$ 1.27 deg
<i>Lemon-balm</i>	40 m	2.12 $\pm$ 1.58 cm	3.21 $\pm$ 2.83 deg

Hence, we evaluated the performance of crop recognition using the similarity distance metric Eq. (2). We do this by evaluating the similarity between different instances of the same crop row (+ve samples) instances of different crop rows (−ve samples) for a range of fields and crop types.

Our results, in Tab. II, highlights the validity of our approach. It can be seen that in all cases the distribution of the +ve and −ve samples is clearly separable. The most challenging crop was beans, where the means were closest and the −ve samples had the largest standard deviation, we attribute this to its cluttered and branchy shape. However, even in this case there is still a clear separation between the +ve and −ve samples. We have also manually measured

TABLE II: Table of the mean ( $\mu$ ) and std. dev ( $\sigma$ ) for the same (+ve) and different (−ve) rows.

Crop	$\mu \pm \sigma$ of +ve cases	$\mu \pm \sigma$ of −ve cases
<i>Beans</i>	0.26 $\pm$ 0.004	0.33 $\pm$ 0.037
<i>Potato</i>	0.15 $\pm$ 0.018	0.27 $\pm$ 0.040
<i>Coriander</i>	0.19 $\pm$ 0.008	0.30 $\pm$ 0.016
<i>Sugar-beet</i>	0.14 $\pm$ 0.014	0.29 $\pm$ 0.015
<i>Lemon-balm</i>	0.20 $\pm$ 0.025	0.29 $\pm$ 0.012

the distance which the robot needed to perform a transition maneuver both in simulation and in the real fields for more than 10 different performances, which outlined an average of 2.1m to 2.6m. By considering the robot’s length being 1.4m, supports our claim that the new lane switching method is requiring less space to be executed.

## VI. CONCLUSION

In this paper, we presented a novel approach to enable autonomous navigation in row-crop fields empowering precision farming and crop monitoring tasks. This approach exploits the crop-row structure using only the local observation from the on-board cameras. Furthermore, it does not require any global or local position awareness for guiding the robot. To achieve this, we have proposed a novel multi-crop-row detection strategy that can deal with cluttered and weedy scenes. We also proposed a novel lane switching strategy which enables BonnBot-I to switch to a new lane independent of any global positioning system or human intervention. This enabled us to perform autonomous field navigation which we evaluated on a robot (BonnBot-I) in the field. Evaluations were performed on BonnBot-I in five different real fields with various crop and canopy types with an average navigation accuracy of 3.82cm.

## ACKNOWLEDGEMENTS

This work was funded by the Deutsche Forschungsgemeinschaft (DFG, German Research Foundation) under Germany’s Excellence Strategy - EXC 2070 – 390732324. This work was also possible with the help of Julius Knechtel and Gereon Tombrink.

## REFERENCES

- [1] "Garford(2014).robocrop inrow weeder," <https://garford.com/>, accessed: 2020-10-22.
- [2] O. Bawden, J. Kulk, R. Russell, C. McCool, A. English, F. Dayoub, C. Lehnert, and T. Perez, "Robot for weed species plant-specific management," *Journal of Field Robotics*, vol. 34, pp. 1179–1199, 2017.
- [3] M. Bakken, V. R. Ponnambalam, R. J. Moore, J. G. O. Gjevestad, and P. J. From, "Robot-supervised learning of crop row segmentation."
- [4] A. Ahmadi, L. Nardi, N. Chebrolu, and C. Stachniss, "Visual servoing-based navigation for monitoring row-crop fields," in *2020 IEEE International Conference on Robotics and Automation (ICRA)*. IEEE, 2020, pp. 4920–4926.
- [5] E. J. Van Henten, J. Hemming, B. Van Tuijl, J. Kornet, J. Meuleman, J. Bontsema, and E. Van Os, "An autonomous robot for harvesting cucumbers in greenhouses," *Autonomous robots*, vol. 13, no. 3, pp. 241–258, 2002.
- [6] M. Pérez-Ruiz, D. C. Slaughter, F. A. Fathallah, C. J. Gliever, and B. J. Miller, "Co-robotic intra-row weed control system," *Biosystems engineering*, vol. 126, pp. 45–55, 2014.
- [7] M. Bayati and R. Fotouhi, "A mobile robotic platform for crop monitoring," *Adv. Robot. Autom.*, vol. 7, no. 2, 2018.
- [8] T. Utstumo, F. Urdal, A. Brevik, J. Dørum, J. Netland, Ø. Overskeid, T. W. Berge, and J. T. Gravdahl, "Robotic in-row weed control in vegetables," *Computers and electronics in agriculture*, vol. 154, pp. 36–45, 2018.
- [9] B. Åstrand and A. J. Baerveldt, "A vision based row-following system for agricultural field machinery," *Mechatronics*, vol. 15, no. 2, pp. 251–269, 2005.
- [10] J. Billingsley and M. Schoenfisch, "The successful development of a vision guidance system for agriculture," *cea*, vol. 16, no. 2, pp. 147–163, 1997.
- [11] B. Thuilot, C. Cariou, P. Martinet, and M. Berducot, "Automatic guidance of a farm tractor relying on a single cp-dgps," *Autonomous robots*, vol. 13, no. 1, pp. 53–71, 2002.
- [12] J. Billingsley and M. Schoenfisch, "The successful development of a vision guidance system for agriculture," *Computers and electronics in agriculture*, vol. 16, no. 2, pp. 147–163, 1997.
- [13] B. Åstrand and A.-J. Baerveldt, "A vision based row-following system for agricultural field machinery," *Mechatronics*, vol. 15, no. 2, pp. 251–269, 2005.
- [14] O. C. Barawid Jr, A. Mizushima, K. Ishii, and N. Noguchi, "Development of an autonomous navigation system using a two-dimensional laser scanner in an orchard application," *Biosystems Engineering*, vol. 96, no. 2, pp. 139–149, 2007.
- [15] F. B. Malavazi, R. Guyonneau, J.-B. Fasquel, S. Lagrange, and F. Mercier, "Lidar-only based navigation algorithm for an autonomous agricultural robot," *Computers and electronics in agriculture*, vol. 154, pp. 71–79, 2018.
- [16] M. Bakken, R. J. Moore, and P. From, "End-to-end learning for autonomous crop row-following," *IFAC-PapersOnLine*, vol. 52, no. 30, pp. 102–107, 2019.
- [17] H. T. Søgård and H. J. Olsen, "Determination of crop rows by image analysis without segmentation," *Computers and electronics in agriculture*, vol. 38, no. 2, pp. 141–158, 2003.
- [18] S. Haug, P. Biber, A. Michaels, and J. Ostermann, "Plant stem detection and position estimation using machine vision," in *Workshop Proc. of Conf. on Intelligent Autonomous Systems (IAS)*, 2014, pp. 483–490.
- [19] H. S. Midtiby, T. M. Giselsson, and R. N. Jørgensen, "Estimating the plant stem emerging points (pseps) of sugar beets at early growth stages," *Biosystems engineering*, vol. 111, no. 1, pp. 83–90, 2012.
- [20] F. Kraemer, A. Schaefer, A. Eitel, J. Vertens, and W. Burgard, "From plants to landmarks: Time-invariant plant localization that uses deep pose regression in agricultural fields," *arXiv preprint arXiv:1709.04751*, 2017.
- [21] V. R. Ponnambalam, M. Bakken, R. J. Moore, J. Glenn Omholt Gjevestad, and P. Johan From, "Autonomous crop row guidance using adaptive multi-roi in strawberry fields," *Sensors*, vol. 20, no. 18, p. 5249, 2020.
- [22] Y.-K. Lin and S.-F. Chen, "Development of navigation system for tea field machine using semantic segmentation," *IFAC-PapersOnLine*, vol. 52, no. 30, pp. 108–113, 2019.
- [23] B. Espiau, F. Chaumette, and P. Rives, "A new approach to visual servoing in robotics," *IEEE Transactions on Robotics and Automation*, vol. 8, no. 3, pp. 313–326, 1992.
- [24] D. A. de Lima and A. C. Victorino, "A visual servoing approach for road lane following with obstacle avoidance," in *17th International IEEE Conference on Intelligent Transportation Systems (ITSC)*. IEEE, 2014, pp. 412–417.
- [25] L. Grimstad and P. J. From, "Thorvald ii-a modular and re-configurable agricultural robot," *IFAC-PapersOnLine*, vol. 50, no. 1, pp. 4588–4593, 2017.
- [26] D. Woebbecke, G. Meyer, K. V. Bargaen, and D. A. Mortensen, "Color indices for weed identification under various soil, residue, and lighting conditions," *Trans. of the American Society of Agricultural Engineers (ASAE)*, vol. 38, no. 1, pp. 259–269, 1995.
- [27] C. Reimann, P. Filzmoser, and R. G. Garrett, "Background and threshold: critical comparison of methods of determination," *Science of the total environment*, vol. 346, no. 1-3, pp. 1–16, 2005.
- [28] J. MacGregor and T. Harris, "The exponentially weighted moving variance," *Journal of Quality Technology*, vol. 25, no. 2, pp. 106–118, 1993.